

ВИСОКОМОЛЕКУЛЯРНІ СПОЛУКИ ТА (НАНО)КОМПОЗИЦІЙНІ МАТЕРІАЛИ

I. Gajdoš¹, J. Slota¹, J. Sikora², V. Krasinskyi³

¹Technical University of Košice, Department of CAx Technologies, Košice, Slovak Republic,

²Lublin University of Technology, Department of Polymer Processing, Lublin, Poland,

³Lviv Polytechnic National University, Department of Chemical Technology of Plastics Processing,
Lviv, Ukraine

EVALUATION OF ROTATIONAL BARREL SEGMENT MIXING PERFORMANCE WITH CFD ANALYSIS

<https://doi.org/10.23939/ctas2020.01.190>

Introducing a new element rotational barrel segment (RBS) into the construction of single screw extruder (SSE) significantly changes kinematic of motion in SSE. The main goal of incorporating RBS into SSE construction is to improve output and mixing capabilities. To evaluate three types of RBS geometries, CAE analysis was performed with ANSYS POLYFLOW® software. Evaluation of three different RBS geometries at two different movement states (screw co-rotating and screw counter-rotating) provided detailed insight in flow phenomena occurring in melted polymer during passing through RBS. CFD simulation of melt flow in SSE allows analyzing various processing conditions, screw geometries and even complicated kinematic couples as screw-RBS.

Key words: rotational barrel segment, mesh superposition technique, ANSYS Polyflow.

Introduction

The single screw extruder (SSE) is one of the most widespread machine types, not only in the plastics and rubber industry but also in other areas such as compounding, food processing, etc. Almost in every polymer processing technology working with the raw materials (injection molding, extrusion, blow molding, etc.), SSE is involved to melt, convey, compress and mix the different compounds. Since their massive development and industrial application during the 20th century, SSE has undergone a continuous growth in all industrial fields, especially in the plastic industry.

The need to speed up of new products development and increase the existent production encourages manufacturers to offer new design solution of SSE. Of course, new solutions were focused on redesigning of the rotary working element (screw) [1], new solutions for heating and cooling the plasticizing system were introduced, but the general design still consisted in placing the screw in a stationary cylinder (barrel).

In 1998 R. Sikora and J.W. Sikora [2] introduced, a new concept of the design of a single screw extruder (SSE). This new design was based on kinematic activation of the barrel itself, which meant it could rotate in the direction identical or opposite to the direction of rotation of the screw (Fig. 1). In this design solution, the barrel of SSE is split into three parts. Two of them are fixed (stationary) parts and a movable part placed between them, adjoining the fixed parts with its end faces and placed inside an outer housing attached to both fixed parts. The movable segment can rotate in the same or opposite direction as the motion of the screw. The rotational barrel segment (RBS) is preferably located in the central part of the plasticizing system and the main goal is to improve mixing capabilities, improve performance and lower the energy consumption of SSE.

Up to date, eight patents cover the RBS design solution, but this concept has not been evaluated in laboratory conditions or implemented in production SSE machines. Construction complexity and high costs related to it present the main issue

that prevented even the production of laboratory-scale SSE. To prove the idea of RBS concept, before a real SSE with this part exists, the application of computer simulation analysis will be used. As a part of tasks solved within NewEX project, the concept of RBS is numerically evaluated, and a new type of SSE with RBS will be built.

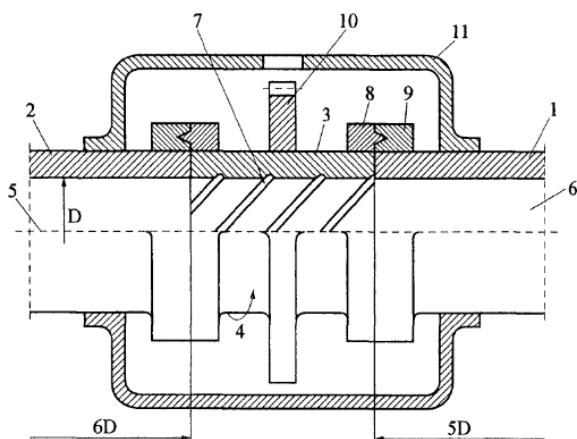


Fig. 1. Rotary sleeve of the plasticizing system's barrel: 1, 2 – fixed parts of the barrel; 3 – rotary element; 4 – direction of rotation of the movable part of the barrel; 5 – screw axis; 6 – inner surface of the fixed part of the barrel; 7 – grooves; 8, 9 – bearings; 10 – gear drive; 11 – external housing

For the screw with simple geometry (one or two continuous flights), numerous researches with numerical 1D models were published e.g. [3–5], calculating melted polymer flow inside an extruder barrel. However, in the case of more complex screw geometry (CRD mixer, pins.), these numerical models encounter their possibilities. Another limitation is that they only provide average numerical values of different parameters along extruder screw that are not sufficient to describe flow pattern and mixing. That is why a 3D CFD FEM simulation for evaluating polymer flow in the extruder barrel is necessary. However, the problem and challenges coupled in such simulations (moving parts, thermal behavior, difficult meshing and remeshing tasks, partial filling, to mention just a few) led to many simplifications of the problem. Simulation with 3D FEM models allows for a more accurate representation of the flow field.

The most proper technique has to combine the power of FEM to deal with strong non-linearities with the simplicity of the mesh generation and absence of remeshing of the BEM. In order to

simplify the setup of a 3D unsteady SSE simulation and to avoid the use of a remeshing algorithm, two techniques referred to as the mesh superposition technique [6] and sliding mesh technique have been implemented in the ANSYS POLYFLOW® software (APF). This robust technique dramatically simplifies the meshing of the geometric entities, avoids the use of any remeshing algorithms and does not present the complexities and limitations of the sliding meshes technique. The mesh superposition technique has three major advantages:

- Mesh generation is much simpler since no complex intermeshing region must be generated.
- It is possible to define a library of moving parts and to combine them with ANSYS Polyfuse to generate new meshes for new simulations.
- The method is robust since no remeshing algorithms are needed and support in APF up to 10 moving parts.

There are also several imitations coupled with this method:

- It can be used only with 2D planar and 3D meshes.
- Allows calculation only with generalized Newtonian flow.
- The detailed variation of the velocity in the neighborhood of the moving part is not well resolved.
- Some fluid leakage can be observed caused by the fact that the physical boundaries do not match finite-element limits, the mass conservation equation cannot be satisfied in every element.

The modeling of internal moving parts requires the modification of the **Navier-Stokes** equations, the mass conservation equation, and possibly the energy equation. The Navier-Stokes equations used in APF to compute a MST task are modified [7]:

$$H(\mathbf{v}-\bar{\mathbf{v}})+(1-H)(-\nabla p+\nabla\cdot\mathbf{T}+\rho\mathbf{g}-\rho\mathbf{a})=\mathbf{0} \quad (1)$$

where: H – is a step function; \mathbf{v} – is the velocity; $\bar{\mathbf{v}}$ – is the local velocity of the moving part; p – is the pressure; \mathbf{T} – is the extra-stress tensor; $\rho\mathbf{g}$ – is the volume force; $\rho\mathbf{a}$ – is the acceleration term

For a generalized Newtonian fluid, the extra-stress tensor is defined to be:

$$\mathbf{T}=2\eta(\dot{\gamma},T)\mathbf{D} \quad (2)$$

where: η – is the viscosity; $\dot{\gamma}$ – is the shear rate; T – is the temperature; \mathbf{D} – is the rate-deformation tensor

Equation 1 is discretized for each node of the velocity field. For node i (at location \mathbf{x}), if it is outside the mesh of moving part, then H is equal to 0 and the usual Navier-Stokes equations are used. Otherwise, H is set to 1, and equation 1 is reduced into:

$$\mathbf{v} = \bar{\mathbf{v}} \quad (3)$$

in order to map the local velocity $\bar{\mathbf{v}}(\mathbf{x})$ of the moving part.

Moreover, before solving the Navier-Stokes equations, the “inner” field H is solved for the melt flow domain. Value of this field can vary from 0 to 1. A flow domain mesh element that is overlapped by the moving part has a value of $H=1$, and the element outside the moving part has a value of $H=0$. A node i (at location \mathbf{x}) is considered to be inside the moving part (that is, $H=1$) if $H(\mathbf{x})$ is greater than a threshold value. The threshold value is usually equal to 0.6, that means that at least 60 % of the elements connected to the node are overlapped by the moving part. Fig. 2 shows a 2D finite element divided into 4 subelements. The subelements that are overlapped by the moving part are marked with a 1, and those that are outside the moving part are marked with a 0.

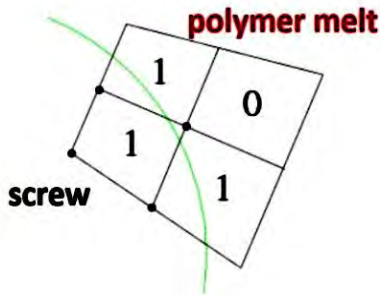


Fig. 2. Presentation of “Inside” Field for a 2D Finite Element

Evaluation of the RBS concept

Purpose of this study is to evaluate the mixing performance of three different RBS concepts, which were designed as a possible solution. For the purposes of this study, the RBS types are identified as concept A, concept B and concept C (fig. 3).

The overall length of solved concepts is $L=200$ mm with barrel diameter $D=25$ mm and with RBS segment placed in the middle of the length. For the concept A and B the RBS segment has a total length of $3D$, whereas for the concept C is the length of RBS designed to $5D$.

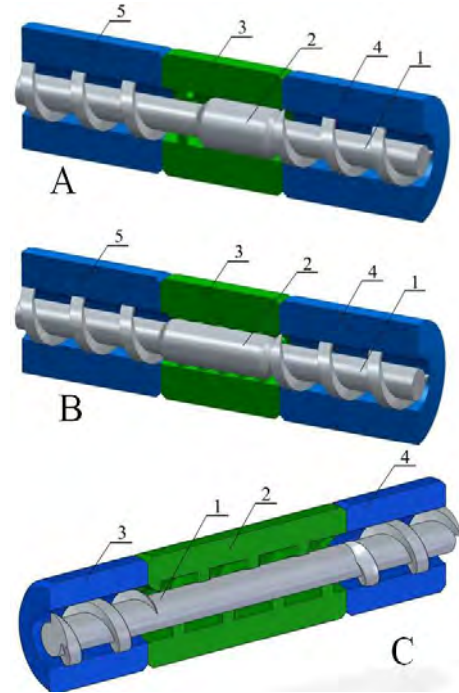


Fig. 3. Design concepts of RBS segments

Mixing performance was evaluated by the value of mixing index (MI) calculated for the flow domain. The mixing index λ is defined as [8]:

$$\lambda = \frac{\dot{\gamma}}{\dot{\gamma} + \omega} \quad (4)$$

where $\dot{\gamma}$ is the equivalent shear rate defined as:

$$\dot{\gamma} = \sqrt{2 \operatorname{tr}(\mathbf{D}^2)} \quad (5)$$

and ω is the magnitude of the vorticity vector. For a shear flow, the mixing index is equal to 0.5, whereas its value is 1 in a purely elongational flow. As the elongational flow is considered more suitable for mixing, value of MI in area of RBS segment will be evaluated to rate the mixing performance.

CFD simulation pre-processing

For the purpose of this study, the models of the proposed RBS concepts were adapted in order to facilitate meshing and reduce the number of mesh elements of rotating parts. A modified model of RBS concept A (RBS and screw) is presented in figure 4. The volume of rotating part was reduced to the necessary minimum. Wall thickness of RBS was left at 1mm. Hole with $\varnothing 10$ mm through the whole length of screw lighted the volume. Concept B and C was modified in a similar way.

Within the CAD software Solidworks®, was also extracted the volume of flow domain prior to meshing (Fig. 5). Prepared models of moving parts

have been subsequently meshed in ANSYS® Fluent® with tetrahedral elements, which are well suited for a complicated geometry. On the other side the flow domain was meshed in ANSYS® Mesh® with prismatic elements to obtain more accurate results in flow calculation. FEM meshes of flow domain and movable parts were subsequently joined in ANSYS Fluent® and exported to ANSYS® Polyflow® (APF).

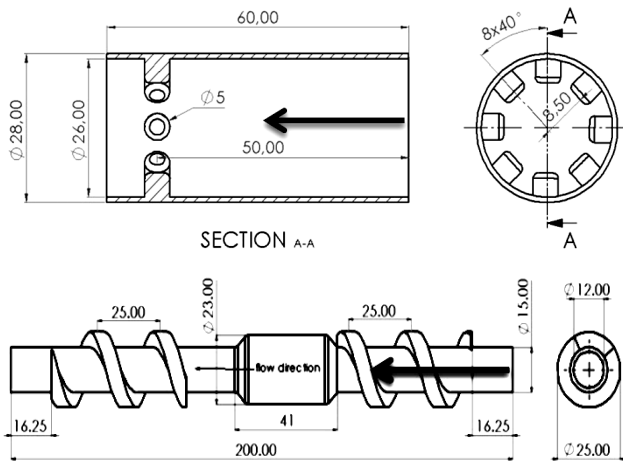


Fig. 4. Drawings of modified RBS (top) and screw for design concept A

Flow calculations in this study were performed in APF, as generalized Newtonian isothermal steady-state. The screw speed was for each type of design concept set to 100 rpm. On the other side for each design concept, two cases of RBS movement were solved. In one case the RBS was rotating in the same direction as the screw, in another case the screw was rotating in the opposite direction always with 100rpm.

Final scheme of the computational problem is shown in Fig. 5, for the RBS concept A. For the concept B and C the values set at boundary conditions remain the same, only the geometry of boundary surfaces changed according to the geometry of moving parts. Flow boundary conditions on the mesh at selected boundaries (BS) were applied:

- BS1 – inflow ($Q = 5.0 \text{ kg/h}$);
- BS2 – normal forces and tangential velocities vanish ($f_n \ \& \ v_s) = (0, 0)$;
- BS3 – cartesian velocities imposed ($v_x \ \& \ v_y \ \& \ v_z) = 10.472 \text{ rad.s}^{-1}$ (100 rpm, direction see Fig. 5);

- BS4 – normal and tangential velocities imposed ($v_n \ \& \ v_s) = (0, 0)$;
- BS5 – cartesian velocities imposed ($v_x \ \& \ v_y \ \& \ v_z) = (10.472 \text{ rad.s}^{-1}$ according to scenario).

The first two boundary conditions, BS1 and BS2, imply that pressure may be generated along the screw. The pressure at the end of the flow domain is unknown, so we calculate the pressure gradient, which is relative to the zero pressure at the flow domain exit. Negative pressures resulting from computations do not mean that negative pressures exist in the extrusion process [9]. Computing negative pressure observed in modeling rotating polymer processing machinery has been described [10].

In this study, the power-law rheological model for the material from the APF database Extrusion_HDPE_isoth_463K was used.

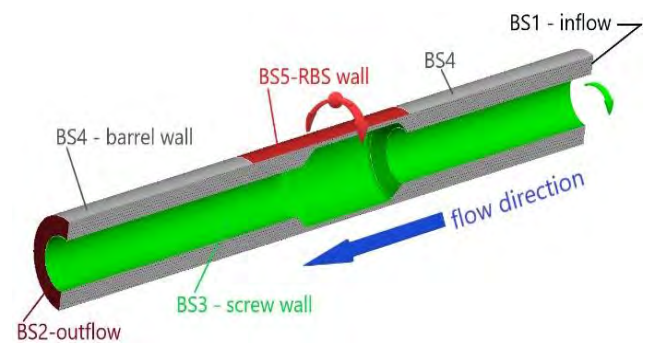


Fig. 5. Longitudinal cross-section through the flow domain CAD model

Simulation results

Flow analysis has been performed for six scenarios of polymer flow through the RBS. MI at the plane going through screw axis is presented in Fig. 6, 7 and 8. Visual comparison of MI map of presented concepts shows a significant impact of RBS rotation direction. When considering mixing performance in all concepts, the mixing performance was better in cases where the RBS rotated in the direction opposite to the screw rotation direction. In the whole flow domain in all concepts and cases, the highest values of the mixing index appeared at the inflow or outflow section. Considering this that those sections are not present in the real extruders (no sudden flight end) and are added to the flow domain to ensure the convergence of calculations, these values should not be taken into account during mixing performance evaluation.

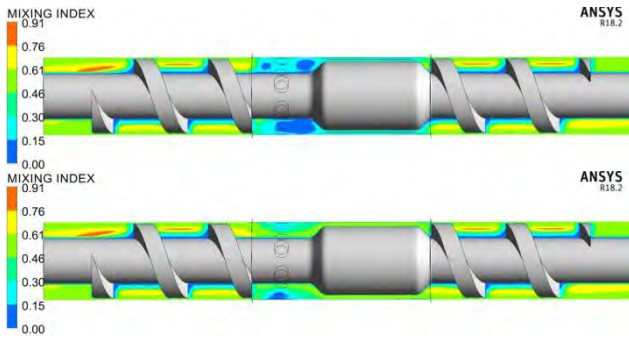


Fig. 6. Values of MI for Concept A with RBS rotating in the same direction as screw (top) and RBS rotating in the opposite direction

In figure 6 is presented MI for Concept A. In the case where the RBS rotates in the same direction, the values of MI are below 0.5 indicating poor mixing performance in RBS area. When the RBS rotates in the opposite direction, MI in RBS area gains values at 0.5–0.6 indicating shear flow. The geometry solution presented in Concept A does not satisfy the demand for improved mixing, as the areas with higher MI are found outside RBS.

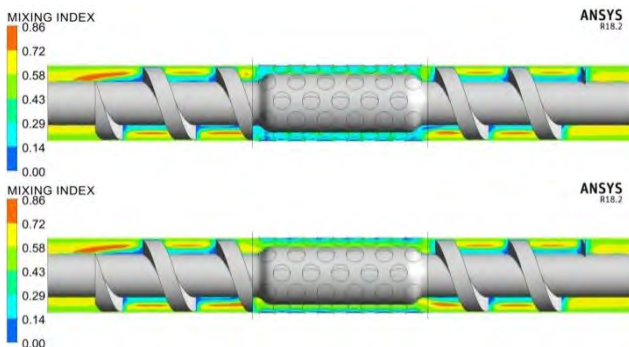


Fig. 7. Values of MI for Concept B with RBS rotating in the same direction as screw (top) and RBS rotating in the opposite direction

Mixing Index for Concept B is presented in Fig. 7. As in the case in the RBC concept A, overall mixing performance is better when RBS is counter-rotating. Values of MI with co-rotating RBS reach maximal values below 0.4. With counter-rotating RBS MI reach values between 0.5–0.7 indicating the presence of shear flow. Areas with 0.86 MI are present in region close to inflow and outflow from RBS section.

Calculated MI in co-rotating Concept C (Fig. 8) shows low or negligible mixing performance, with MI below 0.33. Only small volumes close to screw have MI above 0.5, but not outmatch 0.7 MI. When the RBS is counter-rotating in design Concept C, MI

in area of RBS reaches values above 0.5 indicating better mixing performance.

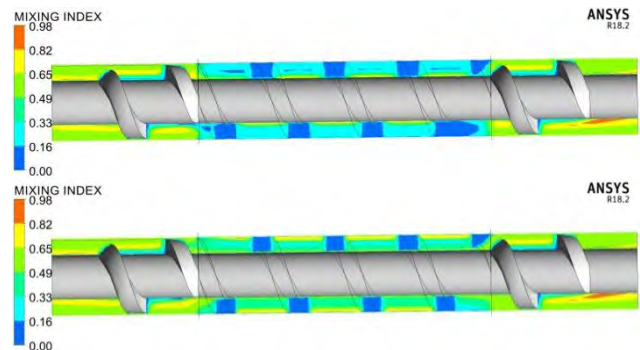


Fig. 8. Values of MI for Concept C with RBS rotating in the same direction as screw (top) and RBS rotating in the opposite direction

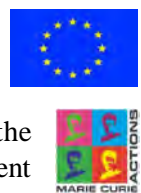
Conclusion

It is highly challenging to prepare simulation task analyzing polymer melt flow inside extruder barrel with complicated geometry shape and two moving parts inside flow domain. In this paper, an approach allowing to calculate mixing performance of new SSE design with RBS is presented. The mixing performance of suggested RBS concepts is evaluated through the value of Mixing Index. Results from the simulation demonstrated that the idea of integrating RBS in extruder construction is correct and investigation of another RBS geometries is necessary to obtain desired performance of SSE equipped with RBS segment, before evaluating RBS in a laboratory environment.

Acknowledgement

The emergence of this article was supported by scientific grant VEGA 1/0259/19

The project leading to this application has received funding from the European Union's Horizon 2020 research and innovation program under the Marie Skłodowska-Curie grant agreement No734205".



References

1. Sikora J. W. (1998). The effect of construction modifications of the extruder barrel grooved zone on the autothermal extrusion process. *Polimery* 43(9), 548–554.
2. Sikora, R. and Sikora, J., (1998). PAT.185728 – *Cylinder of an extrusion machine*, Polish patent – PL 185728.
3. Campbell, G. A., Sweeney, P. A. & Felton, J. N. (1992). Experimental investigation of the drag flow

assumption in extruder analysis. *Polymer Engineering and Science*, 32, 1765–70.

4. Li, Y. and Hsieh F. (1996) Modeling of Flow in a Single Screw Extruder, *Journal of Food Engineering* 27, 353–375.

5. Gaspar-Cunha, A. and Covas, J. A. *Optimization in Polymer Processing*, Nova Science Publishers, (2011).

6. Avalosse, T. (1996). Numerical simulation of distributive mixing in 3-D flows, *Macromolecular Symposia* 112, p. 91.

7. ANSYS Polyflow 2019 R2® online help – <http://ansyshelp.ansys.com>

8. Yang H-H., Manas-Zloczower I. (1994). Analysis of mixing. *International Polymer processing* IX..

9. Wilczynski, K. and Lewandowski, A. (2014). Study on the Polymer Melt Flow in a Closely Intermeshing Counter-Rotating Twin Screw Extruder, *Intern. Polymer Processing* XXIX.

10. Goger, A., Vlachopoulos, J. and Thompson, M. R. (2014). Negative Pressures in Modelling Rotating Polymer Processing Machinery Are Meaningless, But They Are Telling Something, *Int. Polym. Proc.*, 29, 295–297.

І. Гайдос¹, Я. Слота¹, Я. Сікора², В. Красінський³

¹ Технічний університет Кошице, кафедра технологій автоматизованого проектування, Кошице, Словаччина,

² Люблінська політехніка, кафедра переробки полімерів, Люблін, Польща,

³ Національний університет “Львівська політехніка”, кафедра хімічної технології переробки пластмас, Львів, Україна

ОЦІНКА ЗА ДОПОМОГОЮ CFD-МОДЕЛЮВАННЯ ЕФЕКТИВНОСТІ ЗМІШУВАННЯ З ВИКОРИСТАННЯМ ОБЕРТОВОГО СЕГМЕНТА ЦИЛІНДРА

Введення нового обертового сегмента циліндра (ОСЦ) в конструкцію одношнекового екструдера істотно змінює кінематику руху в екструдері. Основна мета включення ОСЦ у конструкцію одношнекового екструдера – підвищення продуктивності та ефективності змішування. Для оцінювання трьох типів геометрії ОСЦ здійснено комп'ютерний аналіз (CAE) за допомогою програмного забезпечення ANSYS POLYFLOW®. Оцінювання трьох різних геометрій ОСЦ у двох різних станах руху (обертання паралельно з шнеком і обертання назустріч шнеку) дала детальну інформацію про явища течії, що виникають у розплавленому полімері під час проходження через ОСЦ. CFD-моделювання течії розплаву в одношнековому екструдері дає змогу аналізувати різні умови переробки, геометрію шнека і навіть складні кінематичні пари, такі як шнек-ОСЦ.

Ключові слова: обертовий сегмент циліндра, техніка суперпозиції сітки, ANSYS Polyflow.